Original scientific paper
DOI: /10.5513/JCEA01/25.3.4342
Journal of Central European Agriculture, 2024, 25(3), p.787-799

Assessment of soil organic matter in the post-fire period using VNIR spectroscopy

Procjena organske tvari tla u razdoblju nakon požara korištenjem VNIR spektroskopije

Iva HRELJA[1] (✉), Igor BOGUNOVIĆ[1], Paulo PEREIRA[2], Ivana ŠESTAK[1]

[1] University of Zagreb Faculty of Agriculture, Department of General Agronomy, Svetošimunska 25, 10000 Zagreb, Croatia
[2] Environment Management Centre, Mykolas Romeris University, Ateities g. 20, LT-08303 Vilnius, Lithuania

✉ Corresponding author: iva.hrelja@gmail.com

Received: March 28, 2024; accepted: July 11, 2024

ABSTRACT

Wildfires profoundly impact ecosystems and soil organic matter (SOM), a critical factor in soil quality and carbon cycling. This research aimed to assess the impact of wildfire severity on SOM and the potential of visible-near infrared spectroscopy (VNIR) spanning the 350 - 1050 nm wavelength range for monitoring SOM in a post-fire landscape using two modelling approaches (i) Partial Least Squares Regression (PLSR) and (ii) Artificial Neural Networks (ANN). Following a comprehensive two-year investigation in Zadar County, Croatia, where a 13.5 ha mixed forest was moderately to severely affected by a wildfire, spectral reflectance analysis revealed that SOM content strongly influenced soil reflectance. High-severity samples exhibited the lowest reflectance compared to those with moderate severity and the control group. The critical region for SOM information in post-wildfire soil estimation models was between 550 and 700 nm. ANN consistently outperformed PLSR, achieving a ratio of performance to deviation (RPD) values from 1.74 to > 2.5. In contrast, PLSR achieved values between 1.62 and 2.29, demonstrating ANN's capability to provide accurate predictions of SOM content in complex post-fire SOM dynamics conditions. This research indicates that VNIR spectroscopy, particularly coupled with ANN-based models, offers a reliable and non-destructive method for assessing SOM content in post-fire environments, facilitating informed land management decisions for ecosystem recovery.

Keywords: wildfire, hyperspectral data, linear modelling, nonlinear modelling

SAŽETAK

Šumski požari imaju dubok utjecaj na ekosustave i organsku tvar tla (eng. SOM), ključni čimbenik kvalitete tla i kruženju ugljika. Cilj ovog istraživanja bio je procijeniti utjecaj jačine šumskog požara na SOM i potencijal vidljivo-blisko infracrvene spektroskopije (eng. VNIR) koja obuhvaća raspon valnih duljina 350 - 1050 nm za praćenje SOM nakon požara koristeći dva pristupa modeliranju (i) Parcijalna regresija najmanjih kvadrata (PLSR) i (ii) Umjetne neuronske mreže (ANN). Nakon sveobuhvatnog dvogodišnjeg istraživanja u Zadarskoj županiji u Hrvatskoj, gdje je 13,5 ha mješovite šume bilo umjereno do jako pogođeno šumskim požarom, analiza spektralne refleksije otkrila je da sadržaj SOM snažno utječe na refleksiju tla. Uzorci visoke jačine pokazali su najnižu refleksiju u usporedbi s onima s umjerenom jačinom i kontrolnom skupinom. Utvrđeno je da je kritično područje za informacije o SOM u modelima procjene tla nakon požara između 550 i 700 nm. ANN je dosljedno nadmašivao PLSR, postigavši vrijednosti omjera performansi i odstupanja (eng. RPD) od 1,74 do > 2,5, dok je PLSR postigao vrijednosti između 1,62 i 2,29, pokazujući sposobnost ANN-a da pruži točna predviđanja sadržaja SOM-a u uvjetima složene dinamike SOM-a nakon požara. Rezultati ovog istraživanja pokazuju da VNIR spektroskopija, posebno u kombinaciji s modelima temeljenim na ANN-u, nudi pouzdanu i nedestruktivnu metodu za procjenu sadržaja SOM nakon požara, olakšavajući informirane odluke o upravljanju zemljištem za oporavak ekosustava..

Ključne riječi: šumski požar, hiperspektralni podaci, linearno modeliranje, nelinearno modeliranje

INTRODUCTION

Increasing problems at the global level, such as unsustainable land management (land-use change, wetland drainage, lack of forest management) and climate change (more frequent weather extremes, higher temperatures, prolonged droughts), are leading to an increase in catastrophic wildfires (Kisić et al., 2023; Ali et al., 2022; Turco et al., 2014). According to the Croatian Fire Brigade (2022), Croatia experienced a 12.11% increase in burned area in 2021, with 37,340 hectares burned, compared to the average from 2011 to 2020. Additionally, in the Mediterranean region of Croatia, the burned area index (the ratio of the burned area to the number of fires) increased by 1.34% in the same year. The increase is to the general predictions that higher temperatures and dryness caused by the variable climatic conditions in this area will create more favourable conditions for the emergence and rapid spread of wildfires in the future (DHMZ - Croatian Meteorological and Hydrological Service, 2013).

Although wildfires of low intensity and severity are part of the natural dynamics of the Mediterranean ecosystem, the recorded more severe wildfires caused by anthropogenic influences and climate change have damaging, often long-lasting, effects on the environment and particularly on soil (Grillakis et al., 2022; Pereira et al., 2019).

High-severity wildfires can cause permanent environmental change, for example, from high-value forests to shrubs, a process which is triggered by post-fire soil erosion (Francos et al., 2018; Sheridan et al., 2018; Verma and Jayakumar, 2015). Additionally, long-term changes include disturbances in soil functions crucial for the survival of the biosphere, such as reduction of nutrient storage capacity, alterations of nutrient cycles, triggering the process of desertification, and modification of organic matter – a key indicator of soil quality (Jiménez-González et al., 2016; Shakesby, 2011; DeBano et al., 1998).

In recent years, the potential of spectral data obtained via field spectroscopy has been explored in soil research, monitoring, and mapping (Šestak et al., 2022; Gholizadeh et al., 2018a). Soil spectroscopy is recognised as a fast, non-destructive and simple analytical method and a tool for comprehensive soil research, which enables the simultaneous evaluation of many soil properties using hyperspectral data, multivariate statistical approaches and chemometric methods (Zovko et al., 2018; Viscarra Rossel et al., 2006).

In recent decades, the use of remote sensing data to monitor the recovery of SOM after wildfires has increased. The development of new technology, such as diffuse visible and near-infrared (VNIR) soil spectroscopy, allowed researchers to gather additional soil data and form complex databases whose information can be used to improve the modelling and prediction of different soil properties, including organic matter (Rosero-Vlasova et al., 2018; Makhamreh, 2006).

VNIR spectroscopy is a type of remote sensing that uses light in the visible and near-infrared spectrum to measure the reflectance of the soil. The reflectance of the soil is dominantly affected by the amount of SOM in the soil, in addition to other soil properties that can affect reflectance, such as soil texture and moisture (Stenberg et al., 2010). Soils with high SOM content tend to be darker in colour and have a lower reflectance than soils with low SOM content. According to Baumgardner et al. (1986), organic matter is one of the most critical properties to explain reflectance differences in the VNIR spectral region arising from the stretching and bending of organic covalent bonds. This information can be used to monitor the recovery of SOM after a wildfire.

Overall, the use of spectroscopy in the VNIR spectrum in combination with multivariate statistical methods has proven to be a precise technique for estimating not just soil C but various other soil properties as well (Viscarra Rossel et al., 2006; Croft et al., 2012). The most commonly used chemometric models are principal component analysis (PCA), stepwise multiple linear regression (SMLR), partial least squares regression (PLSR), principal component regression (PCR), and artificial neural networks (ANN) (Mohamed et al., 2018). Viscarra Rossel and Behrens (2010) compared different modelling algorithms to

determine soil organic carbon content. The ANN model provided the best predictions, mainly because ANNs can model complex nonlinear interactions in the data.

So far, monitoring of spatio-temporal changes in post-fire soil quality has yet to be conducted in the pedological and climatic conditions of Mediterranean Croatia. Therefore, the primary purpose of this research was to apply soil spectroscopy to provide a continuous quantitative assessment of post-fire effects on SOM using two modelling approaches, PLSR and ANN, to facilitate informed land management decisions for ecosystem recovery in Mediterranean conditions.

MATERIALS AND METHODS

Study area and experimental design

The study was conducted in Zadar County, Croatia (44° 05' N; 15° 22' E; 72 m a.s.l), within a 2 km radius of Zadar airport. The climate is Mediterranean (Csa) according to the Köppen-Geiger classification (Kottek et al., 2006), with an average annual temperature of 14.9 °C and precipitation of 879.2 mm. Most of the vegetation in the area consists of *Quercus pubescens* Willd., *Pinus halpensis* Mill., *Pinus pinaster* Ait., *Pinus pinea* L. and *Juniperus communis* L.

The soil type is Cromic Cambisol (IUSS Working Group WRB, 2015). The soil texture is silt loam (Soil Survey Division Staff, 1993). These soils are characterised by their stable aggregate structure, which allows high permeability and good drainage, as well as high content of weatherable minerals, such as feldspars and ferromagnesians (Husnjak, 2014; Chesworth et al., 2008).

The wildfire affected approximately 13.5 ha of a mixed forest of *Quercus pubescens* Willd. and *Juniperus communis* L. on 15 August 2019. The severity of the fire was medium to high, as determined by visual inspection of burned vegetation and ash characteristics (Pereira et al., 2019). The experimental set-up was established according to the characteristics of the burned area, following the methodology described in Pereira et al. (2019): (I) - three categories of sampling areas were defined: C – control (unaffected by fire); MS – medium severity (where foliage and tree trunks were partially burned and soil was covered with black ash); HS – high severity (sites where foliage and tree trunks were completely burned and soil was covered with white ash); (II) - 120 soil samples were collected in total according to severity category (each category contained 40 samples). Finally, each category was subdivided according to the two vegetation species, i.e., each of the three severity categories contained 26 sample areas under *Quercus pubescens* Willd. And 14 sample areas under *Juniperus communis* L. (Figure 1).

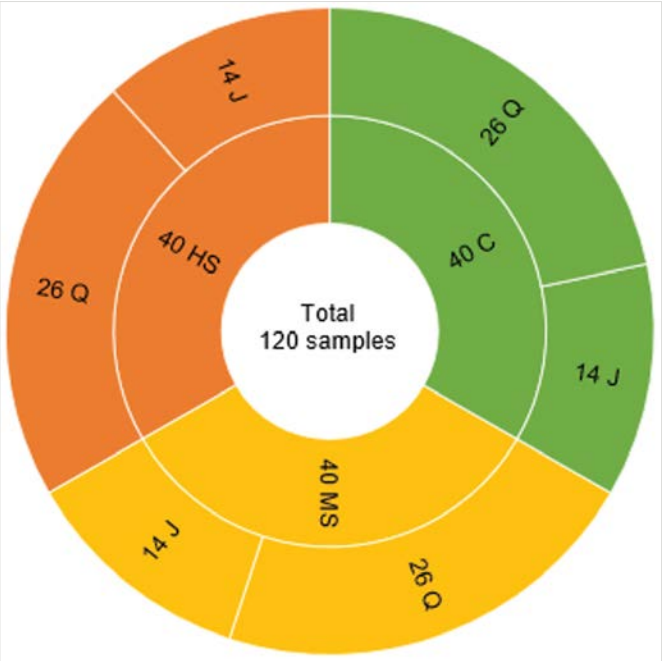

Figure 1. Sample division according to wildfire severity and vegetation type. A total of 120 samples were divided equally into control samples (C) and two wildfire categories: medium severity (MS) and high severity (HS). Each of the three severity categories was further subdivided into samples collected under *Quercus pubescens* Willd (Q) and *Juniperus communis* L. (J)

Prior to the soil sampling procedure, 7 days post-fire, the ash layer on the surface was removed with a soft brush to avoid contamination of the samples and subsequent false results. Afterwards, during the subsequent soil samplings, there was no need for the removal of surface ash because it had already been incorporated into the soil profile via precipitation.

Soil samples were collected at a depth of 0-3 cm with a spade, and each sampling point was georeferenced using a Trimble GeoXH handheld device (GeoExplorer® 6000 series, Trimble GmbH, Raunheim, Germany) and marked with a marking bar. The final experimental design is shown in Figure 2. The markers allowed for periodic soil sampling at the same microsite at seven days (0 MAF), 3 months (3 MAF), 6 months (6 MAF), 9 months (9 MAF), 12 months (12 MAF), 15 months (15 MAF), 18 months (18 MAF), 21 months (21 MAF) and 24 months (24 MAF) post-wildfire within a radius of approximately 0.5 m of the marker. During each sampling campaign, the collection of 120 soil samples was planned, resulting in a total of 1,080 samples.

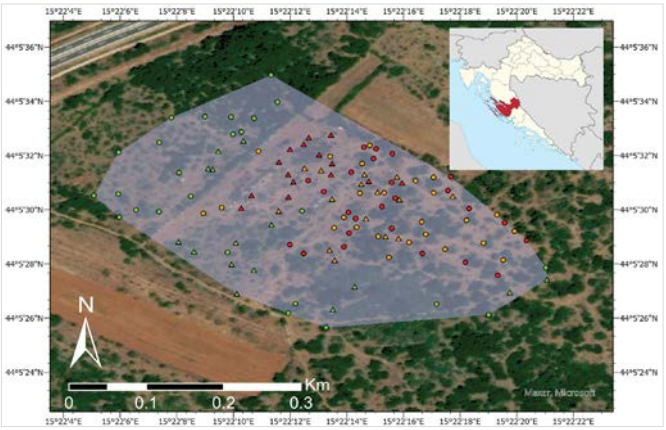

Figure 2. Study area and experimental design. Different shapes denote vegetation species (circles indicate samples under *Quercus pubescens* Willd.; triangles indicate samples under *Juniperus communis* L.), and different colours denote wildfire severity (green - C; orange - MS; red - HS)

Laboratory analysis and measurements of soil reflectance

Per each sampling campaign, 60 air-dried, ground and sieved (<2 mm) samples were separated for chemical analysis, while the remainder of 60 samples were not subjected to chemical analysis. Soil $CaCO_3$ content was determined by volumetric Scheibler calcimeter and total carbon (TC) content by dry combustion using a vario MACRO CHNS analyser (Elementar Analysensysteme GmbH, Langenselbold, Germany). SOM was calculated by multiplying the remainder of the difference between TC and $CaCO_3$ with a factor of 1.724.

Measurement of soil spectral reflectance in laboratory conditions was performed on all air-dried, ground and sieved (<2 mm) samples (N = 120 for each sampling campaign). The measurements were carried out using a portable spectroradiometer (FieldSpec®3, ASD Inc., Boulder, USA) with a wavelength range of 350 - 1050 nm, a sampling interval of 1.4 nm and a spectral resolution of 3 nm with simultaneous recording of 700 wavelengths. Individual soil samples were placed in 1.5 cm petri dishes and recorded at a fixed distance of 0.5 cm using a vertically mounted manual optical probe. Before initial readings, the device was calibrated using a white calibration plate (Spectralon®, Labsphere, North Sutton, USA), and white reference measurements were repeated every 10-15 minutes, per the manufacturer's instructions. The frequency at which the radiation is absorbed gives a reduced reflected signal, registered in the detector as a percentage of reflectance (% R). Each sample's reflectance measurement was taken by averaging 3 consecutive scans to reduce the noise in the spectral signal.

Statistical analysis and model development

Before the statistical analysis was carried out, the collected data were checked for normality using Kolmogorov-Smirnov test. The data was transformed when needed to meet the normality criterion in further statistical analysis using several techniques: logarithmic, Box-Cox and Yeo-Johnson transformations (McGrath et al., 2004; Yeo and Johnson, 2000; Box and Cox, 1964). Z-scores were subsequently calculated to detect outliers, which were removed if the score exceeded 3 standard deviations (Kannan et al., 2015). Once the normalised data were obtained, a one-way analysis of variance (ANOVA) was used to determine the percentage of variation attributable to each factor: sampling time, wildfire severity, and vegetation type. Tukey's HSD test was applied where significant differences were observed ($P < 0.05$).

Raw spectral reflectance data was used in all model developments, and spectral bands from 350 to 409 nm were removed due to the large noise effect. If needed, for improvement of the signal-to-noise ratio, transformations

of the original spectra were performed using first and second derivatives, as well as the Savitzky-Golay filter using a second-order polynomial for derivation and smoothing (Nawar and Mouazen, 2017; Ben-Dor et al., 1997; Savitzky and Golay, 1964).

Two models were compared to develop calibration and validation models for predicting SOM content based on VNIR spectral reflection: (i) linear PLSR and (ii) nonlinear ANN. The independent (predictor, x-variable) input was the raw reflectance data from 410-1050 nm, and the dependent (y-variable) input was the SOM content. The datasets were split into calibration (50%) and validation (50%).

Spectral data were subjected to PCA, a technique that can reduce the dimensionality of a large number of spectral variables, prior to ANN modelling due to its computationally demanding processing time. The PC (principal component) scores obtained via PCA were used as input variables in the ANN modelling procedure.

Models were tested for reliability and prediction ability using full cross-validation. The following coefficient of determination (R^2), root mean square error (RMSE), and the ratio of performance to deviation (RPD) were used to analyse the accuracy and performance of the model. The statistical analysis's significance values were performed for an error probability level of $P < 0.05$. RPD was calculated as the ratio between the standard deviation (SD) of the reference SOM content against the root mean squared error of prediction ($RMSE_p$) and evaluated according to the classification system proposed by Gholizadeh et al. (2018b) (Table 1).

Table 1. Classification system for model accuracy assessment determined by ratio of performance to deviation (RPD) value

RPD value	Classification of the model
< 1.0	very poor
1.0 < RPD < 1.4	poor
1.4 < RPD < 1.8	fair
1.8 < RPD < 2.0	good
2.0 < RPD < 2.5	very good
> 2.5	excellent

RESULTS

Visual soil status report

Figure 3 provides a visual overview of the initial post-fire soil status. By monitoring the vegetation recovery on the study site, it can be stated that vegetation regrowth in MS occurred as early as 3 MAF. Most MS areas affected by the fire in that timeframe exhibited native grass regrowth mixed with other perennial plant species, such as ferns and creepers. On the other hand, HS samples did not follow this trend and were still mostly bare.

In the following vegetation season, 2020, namely on 6 and 9 MAF, MS samples continued to exhibit vegetation regrowth in the form of native grasses. During this time, vegetation started resprouting in HS areas, which mainly consisted of ferns and procumbent/creeper species, but the soil surrounding them was still exposed.

By the 21 and 24 MAF sampling period, MS areas were visually much more comparable to C, while soil in HS areas was still rather exposed (Figure 4).

Soil organic matter content after the wildfire

Throughout the 2-year sampling period, the plan was to collect 120 soil samples per campaign. However, at certain C sampling sites, the unexpectedly dense vegetation at 21 MAF and 24 MAF impeded access to the area, thus preventing sample collection. Consequently, only 1,074 samples were collected out of the intended 1,080 samples.

The Kolmogorov-Smirnov test results showed that the SOM content distribution does not conform to normally distributed data (K-S d = 0.16, *P*-value < 0.001). After the Box-Cox transformation, the Z-scores were calculated, and 2 outliers were detected and removed from further analysis. Normal Gaussian distribution was achieved after transformation, and this dataset was used for further analysis.

The overall SOM content during the study period, according to the severity of the wildfire and vegetation type, is presented in Table 2. Both the standard deviation (SD) and coefficient of variation (CV) indicate moderate

variability in the data set (according to Zhang et al., 2007), especially in the immediate post-fire period (SD = 4.49, CV = 0.53) and at the end of the two-year study (SD = 6.58, CV = 0.55). The average SOM content varied from 6.9 to 11.89% throughout the study. The lowest SOM content of 3.72% was recorded 21 months after wildfire in HS samples and under *Quercus pubescens* Willd. The highest content of 33.19% was recorded 24 months after wildfire in C samples under the same vegetation type.

Analysis of variance revealed that the content in SOM varied significantly over time and according to the severity of wildfire and vegetation type (Table 2). High-severity wildfire caused an overall 21.72% increase in average SOM content, while medium-severity wildfire did not cause a significant change compared to unburned samples (Table 2). In addition, SOM content was significantly higher under *Quercus p.* than *Juniperus c.* throughout the study period (Table 2).

In the first 15 MAFs, HS significantly increased compared to C (Figure 5). The initial (0 MAF) average SOM content in C samples was 7.09%, and the measured content in severely burned areas (0 MAF-HS) was 10.5%, a 48.1% increase. During the following five sampling periods (3, 6, 9, 12 and 15 MAF), the average SOM content in HS was 34.88%, 46.97%, 43.65%, 14.89% and 20.7% higher than content measured in C samples. In the following period (18 and 21 MAF), the content of SOM was higher in HS compared to C, although not significantly. The SOM content in MS showed an 8.68% increase in the immediate post-fire period (0 MAF) compared to C, which is notably lower than the increase observed in HS.

(a) (b) (c)

Figure 3. Soil condition on 22 August 2019 (0 MAF): a) control, b) medium severity, c) high severity

(a) (b) (c)

Figure 4. Soil condition on 26 August 2021 (24 MAF): a) control, b) medium severity, c) high severity

Table 2. Descriptive statistics of SOM content (%) and ANOVA results for nine sampling times, three wildfire severity levels and two vegetation types

	Sampling time									Wildfire severity			Vegetation	
	0 MAF	3 MAF	6 MAF	9 MAF	12 MAF	15 MAF	18 MAF	21 MAF	24 MAF	C	MS	HS	*Quercus* p.	*Juniperus* c.
N	60	60	60	60	60	60	60	56	59	178	179	178	348	187
Mean	8.54^{b}	7.30^{b}	7.92^{b}	7.42^{b}	6.90^{b}	7.38^{b}	7.80^{b}	7.01^{c}	11.89^{a}	7.55^{b}	7.31^{b}	9.19^{a}	8.94^{a}	7.04^{b}
Min	4.68	4.52	4.21	4.01	4.44	4.38	4.03	3.72	4.99	4.01	4.00	3.72	3.72	4.00
Max	23.89	20.34	22.80	17.92	12.93	15.94	16.07	21.85	33.19	33.19	22.96	31.76	33.19	27.99
SD	4.49	2.81	3.28	2.65	2.13	2.37	2.51	3.20	6.58	3.58	2.80	4.64	3.97	3.33
CV	0.53	0.38	0.41	0.36	0.31	0.32	0.32	0.46	0.55	0.47	0.38	0.50	0.44	0.47

MAF – Months after fire; C – Control; MS – Medium severity; HS – High severity; SD – Standard deviation; CV – Coefficient of variation. Different letters represent significant ($P < 0.05$) differences among sampling times, wildfire severities, and vegetation types.

No significant change compared to C was recorded during the 3, 6, 12, 15, 18 and 21 MAF. On the final sampling date (24 MAF), MS showed a 29.97% decrease in average SOM content compared to C, with no significant difference between C and HS samples.

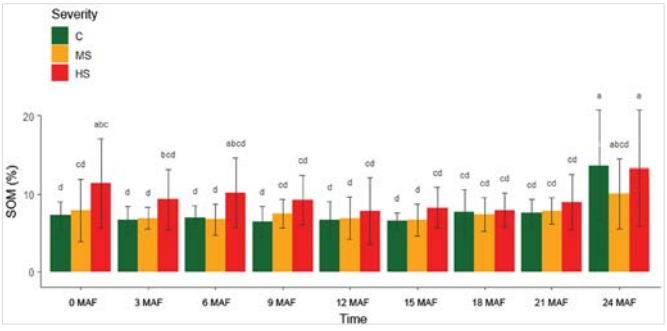

Figure 5. Mean SOM content (%) according to the interaction of the wildfire severity and time-since-fire factors. Whiskers represent standard deviation. Different letters indicate significant ($P < 0.05$) differences between wildfire severity and time-since-fire

Soil spectral data

The average spectral data of three wildfire severities were grouped according to vegetation and sampling time. Figures 6 - 9 compare the average reflectance of C, MS, and HS taken under *Juniperus* c. and *Quercus* p. at the study period's beginning and end (0 MAF and 24 MAF). In the immediate post-fire period (0 MAF), the greatest spectral differences between C, MS, and HS groups were in the green/yellow to red (550 to 700 nm) region, especially in samples taken under *Quercus* p. vegetation (Figure 7b).

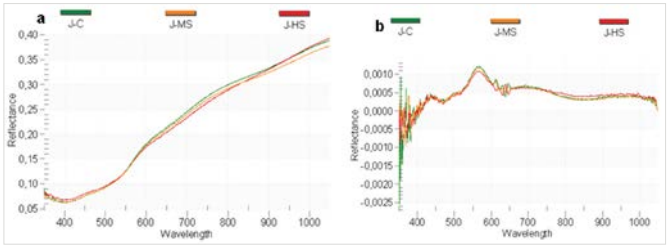

Figure 6. Average raw (a) and first derivative (b) reflectance for control, medium severity and high severity samples taken under *Juniperus* c. vegetation immediately post-fire at 0 MAF (N = 42). Wavelengths are expressed in nm.

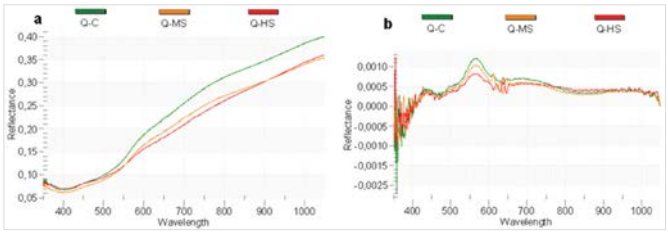

Figure 7. Average raw (a) and first derivative (b) reflectance for control, medium severity and high severity samples taken under *Quercus* p. vegetation immediately post-fire at 0 MAF (N = 78). Wavelengths are expressed in nm.

At the end of the study period (24 MAF), these spectral differences remained visible between the C and HS groups. However, MS exhibited higher reflectance throughout the entire spectra, which was visible in both vegetation species (Figures 8 and 9).

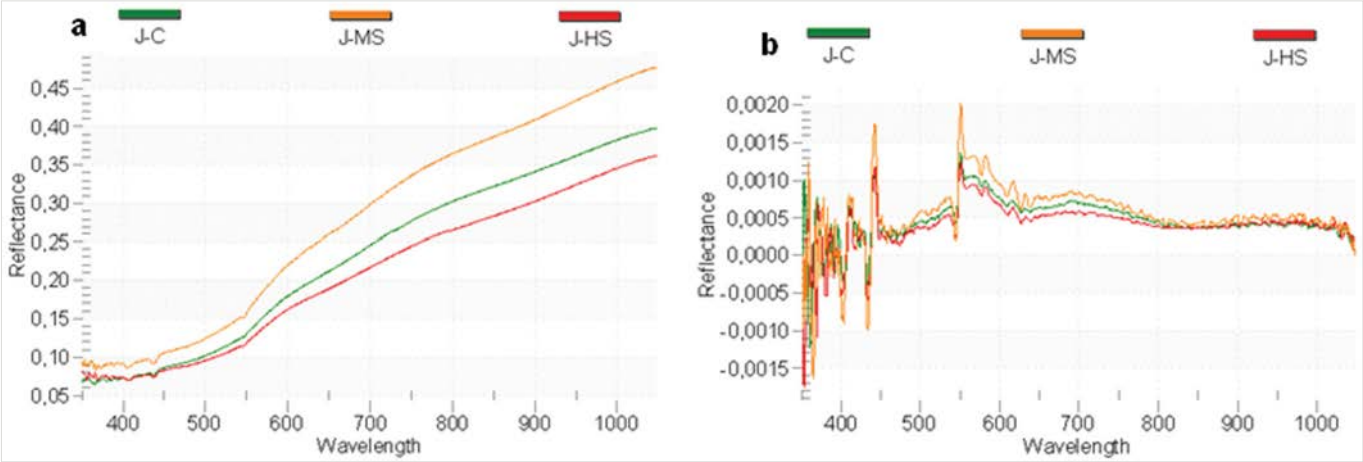

Figure 8. Average raw (a) and first derivative (b) reflectance for control, medium severity and high severity samples taken under *Juniperus* c. vegetation two years post-fire at 24 MAF (N = 42). Wavelengths are expressed in nm.

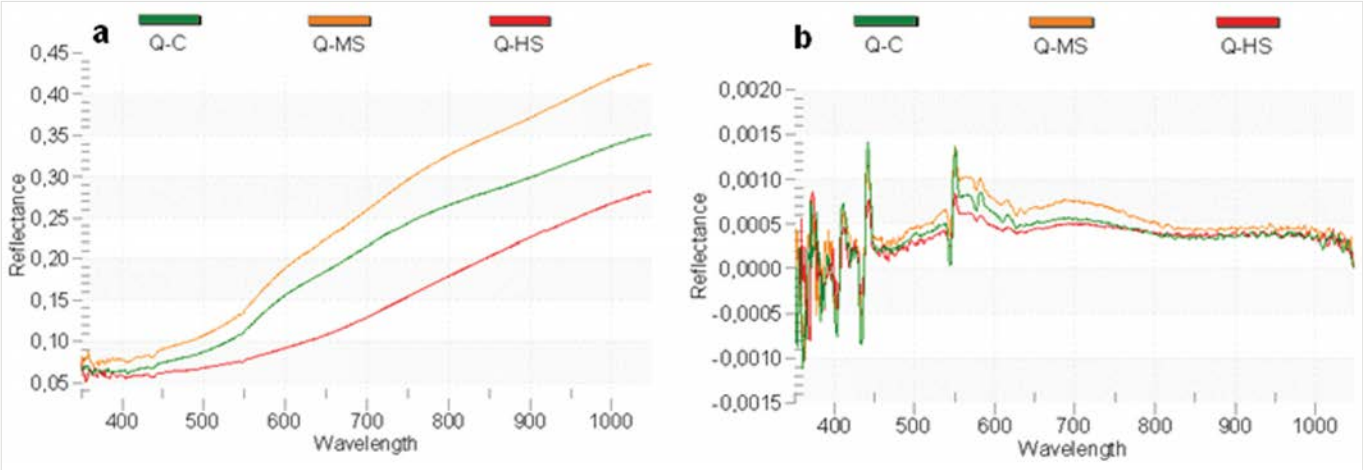

Figure 9. Average raw (a) and first derivative (b) reflectance for control, medium severity and high severity samples taken under *Quercus* p. vegetation two years post-fire at 24 MAF (N = 78). Wavelengths are expressed in nm.

Comparison of PLSR and ANN models

Spectral bands from 350 to 409 nm were removed from further analysis due to the large noise effect that can be seen best from the first derivative reflectances (Figures 6b, 7b, 8b and 9b). In each PLSR model, three to five PCs were identified that represented the primary structured information in the spectral dataset (Table 3).

PLSR models computed for each sampling time provided fair to very good predictions according to RPD, with values ranging from 1.62 (6 MAF) to 2.29 (21 MAF), with an exception at 3 MAF which produced a poor model (RPD = 1.35) (Table 3). 3 MAF model was the only model that benefited from the data smoothing procedure (Savitzky-Golay). The PLSR model computed for the entire dataset collected over the study period (ALL MAF) provided fair predictions, with an RPD value of 1.55 (Table 3).

For ANN modelling, the input predictors (x-variables) were the PCA scores of raw reflectance data. Eleven to eighteen PCs summarised the most variation in the reflectance datasets (Table 3). RPD values of ANN outperformed PLSR models, with RPD values ranging from 1.96 (9 MAF) to >2.5 (0, 3, 15, 18 and 24 MAF), which all fall in the category of very good and excellent models (Table 3). One exception was the model obtained at 21 MAF when PLSR outperformed ANN with an RPD value of 2.29 (21 MAF ANN RPD = 1.74).

Table 3. PLSR and ANN Model performance at each individual sampling period and for the entire reflectance dataset

Dataset summary						Model performance					
MIN	MAX	MEAN	SD	CV		NPC	$RMSE_C$	$RMSE_P$	R^2_C	R^2_P	RPD
0 MAF (N=119)											
4.68	23.89	8.60	4.12	0.48	PLSR	4	1.66	1.95	0.84	0.78	2.11
					ANN	11	0.41	0.82	0.99	0.96	>2.5
3 MAF (N=120)											
4.52	20.34	7.65	2.81	0.37	PLSR	3	1.63	2.08	0.66	0.46	1.35
					ANN	13	1.34	1.09	0.77	0.85	>2.5
6 MAF (N=120)											
4.21	22.80	7.97	3.28	0.41	PLSR	3	1.8	2.02	0.69	0.62	1.62
					ANN	14	1.14	1.5	0.88	0.79	2.18
9 MAF (N=120)											
4.01	17.44	7.55	2.31	0.31	PLSR	5	1.19	1.35	0.73	0.66	1.71
					ANN	13	0.95	1.18	0.83	0.74	1.96
12 MAF (N=120)											
4.44	12.93	7.14	2.13	0.30	PLSR	3	1.14	1.26	0.71	0.66	1.69
					ANN	11	0.88	0.93	0.83	0.81	2.29
15 MAF (N=120)											
4.38	15.94	7.69	2.37	0.31	PLSR	4	1.08	1.18	0.79	0.76	2.01
					ANN	14	0.82	0.34	0.88	0.98	>2.5
18 MAF (N=120)											
4.03	16.07	8.14	2.51	0.31	PLSR	4	1.03	1.13	0.83	0.8	2.22
					ANN	13	0.5	0.94	0.96	0.86	>2.5
21 MAF (N=120)											
3.72	21.85	7.12	3.20	0.45	PLSR	3	1.21	1.4	0.86	0.82	2.29
					ANN	18	0.64	1.84	0.96	0.67	1.74
24 MAF (N=118)											
4.99	33.19	12.08	6.34	0.52	PLSR	4	2.84	3.29	0.8	0.73	1.93
					ANN	18	0.9	2	0.98	0.9	>2.5
ALL MAF (N=1074)											
3.72	33.19	8.33	3.86	0.46	PLSR	4	2.44	2.49	0.59	0.57	1.55
					ANN	15	1.85	2.15	0.77	0.69	1.79

SD – Standard deviation; CV – Coefficient of variation; NPC – optimal number of principal components; $RMSE_C$ – Root mean square error of calibration; $RMSE_P$ – Root mean square error of prediction; R^2_C – Coefficient of determination for calibration; R^2_P – Coefficient of determination for validation; RPD – Ratio of performance to deviation

DISCUSSION

Impacts of wildfire severity on SOM content

A significant increase in SOM content in the HS samples compared to MS and C was recorded in the first 9 MAF (by 35 to 48%), which indicated that incorporation of burned material (ash, charred foliage and bark, dead roots, burned grass-bed) into the soil profile occurred. In the following period of 12-21 MAF, the SOM content in HS was still elevated compared to C, although not significantly (Figure 5), probably because of an onset of slow vegetation regrowth and recovery, which was first observed in HS in the study field in the spring following the wildfire (6 MAF). However, as visually confirmed during the entire 2-year study period, the vegetation recuperation in HS was slower than in MS, which certainly caused reduced nutrient demand and uptake. This probably resulted in the accumulation of soil nutrients and SOM.

The increase in post-fire SOM was also reported by Muráňová and Šimanský (2015), who recorded a 24% increase in SOC content in HS in the immediate post-fire period. Interestingly, they reported an increase in the amount of post-fire SOC content, but at the same time, its quality worsened due to the deterioration of the humic to fulvic acid ratio. Unfortunately, this study did not address the detailed breakdown and the nature of post-fire SOM and is, in this sense, limited to extrapolating some deductions based solely on measures of increase or decrease of SOM. Future studies should further investigate the nature of post-fire SOM in terms of its quality to confirm or deny the findings reported in this study.

SOM content in MS increased significantly (by ~9%) in the immediate post-fire period (0 MAF). It was higher than in C in the following post-fire period (although not significantly), suggesting that the incorporation of burned material occurred but was not as pronounced as in HS. Additionally, the recuperation of vegetation on all MS sites was visible as early as 3 MAF, possibly due to the overall lower temperature reached during a wildfire on these sites coupled with partial combustion of biomass, which resulted in more favourable conditions for vegetation recovery. This supports the previous studies that low and medium-severity wildfires generally have a more neutral or even beneficial effect on ecosystem recovery compared to high-severity wildfires (Yang et al., 2021; Pereira et al., 2017; Alcañiz et al., 2016; Inbar et al., 2014).

At 24 MAF, a significantly lower SOM content recorded in MS compared to C indicated intensive and ongoing vegetation regeneration in these areas affected by a wildfire of lower severity, as supported via visual observations of post-fire vegetation recovery of the wildfire-affected area and observed in previous studies (Fuentes-Ramirez et al., 2022; Arroyo-Vargas et al., 2019).

Impacts of wildfire severity on soil reflectance

As shown in Figures 6 - 9, differences in spectral curve behaviour between two wildfire severities and control are evident in both vegetation species. Specifically, HS samples had the highest average SOM content and, therefore, the lowest average reflectance throughout the study period. In contrast, C samples had the lowest average SOM content, causing the highest average reflectance. At 0 MAF, the green/yellow to red reflectance region (550 to 700 nm) decreased in burned areas. Similar results were obtained by Šestak et al. (2022), who reported a decrease in soil reflectance following wildfire in the same reflectance region on burned samples from Mediterranean Croatia. These results support that SOM differences explain reflectance variation in the VNIR spectral region, namely, higher SOM content decreases reflectance and vice versa (Baumgardner et al.,1986). According to Zheng et al. (2016) and Tian et al. (2013), SOM content correlates with reflectance in the range from 500-700 nm the most. These observations in research conducted on various soil types, including this study, lead to a conclusion that the 550-700 nm range carries most of the information on SOM that could be useful in developing universal models for estimating SOM in different types of soils, including ones affected by wildfires. Higher reflectance recorded at 24 MAF in MS samples compared to both C and HS supports the

assumption of intensive vegetation regeneration during this period, favouring mineralisation of SOM and nutrient uptake, as previously discussed.

Comparison of PLSR and ANN models

3 MAF PLSR was the only model that benefited from a data smoothing procedure that effectively preserved high-frequency signal components and reduced noise. However, a large part of the variation in the model still remains unexplained. This is probably related to the complex wildfire impacts on SOM and the effects of intrinsic factors that occurred in the immediate post-fire period. Namely, according to Cofer et al. (1997), vegetation wildfires lead to the formation of char and new forms of C that could have affected the linear VNIR-SOM relationship and behavior of spectral curves. The ongoing complex processes of post-fire soil recovery clearly show a nonlinear relationship, as observed in other studies (Pereira et al., 2019; Francos et al., 2018; Prendergast-Miller et al., 2017). This is why nonlinear ANN models generally proved superior to PLSR models. These results confirm that learning nonlinear ANN algorithms can correlate complex spectral information with the target variable, especially in complex post-fire SOM dynamics conditions. Similar results were obtained by Viscarra Rossel and Behrens (2010), who compared multiple data mining techniques, including PLSR and ANN, for calibrating VNIR reflectance spectra to SOC and confirmed the superiority of the ANN model that can detect complex nonlinear interactions in the data.

As for the PLSR model obtained with the entire 0-24 MAF dataset, its accuracy and performance were inferior to individual models computed for each sampling period separately, with $RMSE_p$ of 2.49, R^2 of 0.57 between measured and predicted SOM content, and RPD value of 1.55 indicating a fair model. These results emphasise the benefit of data segmentation during the short-term post-wildfire monitoring that enables us to model specific features of post-fire SOM dynamics. It is beneficial for post-fire SOM monitoring to use models computed according to the specific stages of SOM dynamics, i.e. to compute models segmented by the rate of soil regeneration and/or seasonal criteria that consider the speed and seasonality of soil changes. However, to reduce costs, a generalised model based on all available data could be useful to detect SOM recovery's direction.

CONCLUSIONS

The spectral reflectance analysis revealed that soil reflectance is significantly affected by variations in SOM content resulting from different wildfire severities. The greatest spectral differences between C, MS and HS were found in the green/yellow to red (550-700 nm) region. This suggests that this region carries most of the information on SOM that could be useful in developing universal models for estimating SOM in soils affected by wildfires. Nonlinear models such as ANN should be used to estimate the field variability of SOM, especially in the complex conditions of post-fire soil dynamics.

The data acquired and analysed in this study provided short-term information on wildfire effects on SOM content on a local scale and provided some valuable insights into the direction of SOM recovery in the Mediterranean environment. Long-term studies (10-30 years) are encouraged to develop models that monitor the effects on SOM and to fully understand the spatial and temporal change in soil quality.

ACKNOWLEDGEMENTS

The content of this paper has been previously published as part of the doctoral thesis titled 'Spatio-temporal dynamic of soil organic matter in fire affected land using spectroscopy and remote sensing' authored by Iva Hrelja, submitted to the University of Zagreb Faculty of Agriculture in 2024. The thesis was defended on 19 March 2024, and is stored in the National and University Library in Zagreb, Ulica Hrvatske bratske zajednice 4 p.p. 550, 10 000 Zagreb, and Library of the University of Zagreb, Faculty of Agriculture, Svetošimunska cesta 25, 10 000 Zagreb.

The authors extend their gratitude to Associate Professor Aleksandra Perčin for her assistance with the laboratory analysis.

REFERENCES

Alcañiz, M., Outeiro, L., Francos, M., Farguell, J., Úbeda, X. (2016) Long-term dynamics of soil chemical properties after a prescribed fire in a Mediterranean forest (Montgrí Massif, Catalonia, Spain). Science of The Total Environment, 572, 1329–1335. DOI: https://doi.org/10.1016/j.scitotenv.2016.01.115

Ali, E., Cramer, W., Carnicer, J., Georgopoulou, E., Hilmi, N.J.M., Le Cozannet, G., Lionello, P. (2022) Cross-Chapter Paper 4: Mediterranean Region. In: Pörtner, H.O., Roberts, D.C., Tignor, M., Poloczanska, E.S., Mintenbeck, K., Alegría, A., Craig, M., Langsdorf, S., Löschke, S., Möller, V., Okem, A., Rama, B., eds. Climate Change 2022: Impacts, Adaptation, and Vulnerability. Contribution of Working Group II to the Sixth Assessment Report of the Intergovernmental Panel on Climate Change. Cambridge University Press, pp. 2233–2272.

Arroyo-Vargas, P., Fuentes-Ramírez, A., Muys, B., Pauchard, A. (2019) Impacts of fire severity and cattle grazing on early plant dynamics in old-growth Araucaria-Nothofagus forests. Forest Ecosystems, 6 (1), 44. DOI: https://doi.org/10.1186/s40663-019-0202-2

Baumgardner, M.F., Silva, L.F., Biehl, L.L., Stoner, E.R. (1986) Reflectance Properties of Soils. Advances in Agronomy, 38, 1–44. DOI: https://doi.org/10.1016/S0065-2113(08)60672-0

Ben-Dor, E., Inbar, Y., Chen, Y. (1997) The reflectance spectra of organic matter in the visible near-infrared and short wave infrared region (400–2500 nm) during a controlled decomposition process. Remote Sensing of Environment, 61 (1), 1–15. DOI: https://doi.org/10.1016/S0034-4257(96)00120-4

Box, G.E.P., Cox, D.R. (1964) An Analysis of Transformations. Journal of the Royal Statistical Society: Series B (Methodological), 26 (2), 211–243. DOI: https://doi.org/10.1111/j.2517-6161.1964.tb00553.x

Chesworth, W., Camps Arbestain, M., Macías, F., Spaargaren, O., Spaargaren, O. (2008) Cambisols. In: Chesworth, W., ed. Encyclopedia of Soil Science, Encyclopedia of Earth Sciences Series. Dordrecht: Springer, pp. 80–81. DOI: https://doi.org/10.1007/978-1-4020-3995-9_85

Cofer, W.R., Koutzenogii, K.P., Kokorin, A., Ezcurra, A. (1997) Biomass Burning Emissions and the Atmosphere. In: Clark, J.S., Cachier, H., Goldammer, J.G., Stocks, B., eds. Sediment Records of Biomass Burning and Global Change. Berlin, Heidelberg: Springer, pp. 189–206. DOI:10.1007/978-3-642-59171-6_9

Croatian Fire Brigade (2022) Statistical report of the State's Fire Operations Center 193 with an overview of fire data for 2022. Available at: https://hvz.gov.hr/ [Accessed 31 March 2022].

Croft, H., Kuhn, N. J., Anderson, K. (2012) On the use of remote sensing techniques for monitoring spatio-temporal soil organic carbon dynamics in agricultural systems. Catena, 94, 64-74. DOI: https://doi.org/10.1016/j.catena.2012.01.001

DeBano, L. F., Neary, D. G., Ffolliott, P. F. (1998). Fire effects on ecosystems. John Wiley & Sons, New York, USA, pp. 1-13.

DHMZ – Croatian Meteorological and Hydrological Service (2013) Sixth National Communication of the Republic of Croatia under the United Nation Framework Convention on the Climate Change (UNFCCC). Available at: https://klima.hr/razno/publikacije/NIKP6_DHMZ.pdf [Accessed 07 April 2022]

Francos, M., Úbeda, X., Pereira, P., Alcañiz, M. (2018) Long-term impact of wildfire on soils exposed to different fire severities. A case study in Cadiretes Massif (NE Iberian Peninsula). Science of the Total Environment, 615, 664-671. DOI: https://doi.org/10.1016/j.scitotenv.2017.09.311

Fuentes-Ramirez, A., Almonacid-Muñoz, L., Muñoz-Gómez, N., Moloney, K.A. (2022) Spatio-Temporal Variation in Soil Nutrients and Plant Recovery across a Fire-Severity Gradient in Old-Growth Araucaria-Nothofagus Forests of South-Central Chile. Forests 13 (3), 448. DOI: https://doi.org/10.3390/f13030448

Gholizadeh, A., Saberioon, M., Ben-Dor, E., Borůvka, L. (2018a) Monitoring of selected soil contaminants using proximal and remote sensing techniques: Background, state-of-the-art and future perspectives. Critical reviews in environmental science and technology, 48 (3), 243-278.

Gholizadeh, A., Žižala, D., Saberioon, M., Borůvka, L. (2018b) Soil organic carbon and texture retrieving and mapping using proximal, airborne and Sentinel-2 spectral imaging. Remote Sensing of the Environment, 218, 89–103.

Grillakis, M., Voulgarakis, A., Rovithakis, A., Seiradakis, K.D., Koutroulis, A., Field, R.D., Kasoar, M., Papadopoulos, A., Lazaridis, M. (2022) Climate drivers of global wildfire burned area. Environmental Research Letters, 17 (4), 045021.

Husnjak, S. (2014) Soil systematics of Croatia. University textbook, Zagreb: University of Croatia publishing house.

Inbar, A., Lado, M., Sternberg, M., Tenau, H., Ben-Hur, M. (2014) Forest fire effects on soil chemical and physicochemical properties, infiltration, runoff, and erosion in a semiarid Mediterranean region. Geoderma, 221–222, 131–138. DOI: https://doi.org/10.1016/j.geoderma.2014.01.015

IUSS Working Group WRB (2015) World Reference Base for Soil Resources 2014, update 2015. International soil classification system for naming soils and creating legends for soil maps. World Soil Resources Reports, No. 106. FAO, Rome.

Jiménez-González, M.A., De la Rosa, J.M., Jiménez-Morillo, N.T., Almendros, G., González-Pérez, J.A., Knicker, H. (2016) Post-fire recovery of soil organic matter in a Cambisol from typical Mediterranean forest in Southwestern Spain. Science of The Total Environment, 572, 1414–1421. DOI: https://doi.org/10.1016/j.scitotenv.2016.02.134

Kannan, K. S., Manoj, K., Arumugam, S. (2015). Labeling methods for identifying outliers. International Journal of Statistics and Systems, 10(2), 231-238.

Kisić, I., Bogunović, I., Delač, D., Barčić, D. (2023) Open space fires in the Republic of Croatia - occurrence, frequency and suppression. Hrvatske vode, 31 (124), 117-126.

Kottek, M., Grieser, J., Beck, C., Rudolf, B., Rubel, F. (2006) World map of the Köppen-Geiger climate classification updated. Meteorologische Zeitschrift, 15 (3), 259-263.

Makhamreh, Z. (2006) Evaluation of soil quality and development stage using spectral reflectance of soils: Case Study in Eastern Mediterranean region. In Proceedings of the International Conference: Soil and Desertification–Integrated Research for the Sustainable Management of Soils in Drylands. Hamburg, Germany, 5-6 May, 1-7.

McGrath, D., Zhang, C., Carton, O.T. (2004) Geostatistical analyses and hazard assessment on soil lead in Silvermines area, Ireland. Environmental Pollution, 127 (2), 239–248. DOI: https://doi.org/10.1016/j.envpol.2003.07.002

Mohamed, E. S., Saleh, A. M., Belal, A. B., Gad, A. (2018). Application of near-infrared reflectance for quantitative assessment of soil properties. The Egyptian Journal of Remote Sensing and Space Science, 21(1), 1-14. DOI: https://doi.org/10.1016/j.ejrs.2017.02.001

Muráňová, K., Šimanský, V. (2015) The effect of different severity of fire on soil organic matter and aggregates stability. Acta fytotechnica et zootechnica, 18 (1), 1-5. DOI: https://doi.org/10.15414/afz.2015.18.01.01-05

Nawar, S., Mouazen, A.M. (2017) Predictive performance of mobile vis-near infrared spectroscopy for key soil properties at different geographical scales by using spiking and data mining techniques. CATENA, 151, 118–129. DOI: https://doi.org/10.1016/j.catena.2016.12.014

Pereira, P., Brevik, E. C., Bogunović, I., Estebaranz-Sánchez, F. (2019). Ash and soils. A twin relationship in fire-affected areas. In: Pereira, P., Mataix-Solera, J., Úbeda, X., Reind, G., Cerdà, A., eds. Fire effects on soil properties. Leiden: CSIRO Publishing, pp. 39-67.

Pereira, P., Cerda, A., Martin, D., Úbeda, X., Depellegrin, D., Novara, A., Martínez-Murillo, J.F., Brevik, E.C., Menshov, O., Comino, J.R., Miesel, J. (2017). Short-term low-severity spring grassland fire impacts on soil extractable elements and soil ratios in Lithuania. Science of The Total Environment, 578, 469–475. DOI: https://doi.org/10.1016/j.scitotenv.2016.10.210

Prendergast-Miller, M.T., de Menezes, A.B., Macdonald, L.M., Toscas, P., Bissett, A., Baker, G., Farrell, M., Richardson, A.E., Wark, T., Thrall, P.H. (2017) Wildfire impact: Natural experiment reveals differential short-term changes in soil microbial communities. Soil Biology and Biochemistry, 109, 1–13. DOI: https://doi.org/10.1016/j.soilbio.2017.01.027

Rosero-Vlasova, O.A., Vlassova, L., Pérez-Cabello, F., Montorio, R., Nadal-Romero, E. (2018) Modelling soil organic matter and texture from satellite data in areas affected by wildfires and cropland abandonment in Aragón, Northern Spain. Journal of Applied Remote Sensing, 12 (4), 042803. DOI: https://doi.org/10.1117/1.JRS.12.042803

Savitzky, A., Golay, M.J.E. (1964) Smoothing and Differentiation of Data by Simplified Least Squares Procedures. Analytical Chemistry, 36 (8), 1627–1639. DOI: https://doi.org/10.1021/ac60214a047

Šestak, I., Pereira, P., Telak, L.J., Perčin, A., Hrelja, I., Bogunović, I. (2022) Soil Chemical Properties and Fire Severity Assessment Using VNIR Proximal Spectroscopy in Fire-Affected Abandoned Orchard of Mediterranean Croatia. Agronomy, 12 (1), 129. DOI: https://doi.org/10.3390/agronomy12010129

Shakesby, R.A. (2011) Post-wildfire soil erosion in the Mediterranean: Review and future research directions. Earth-Science Reviews, 105 (3–4), 71–100. DOI: https://doi.org/10.1016/j.earscirev.2011.01.001

Sheridan, G., Lane, P., Nyman, P. (2018) Erosion. In: Pereira, P., Mataix-Solera, J., Úbeda, X., Rein, G., Cerdà, A., eds. Fire Effects on Soil Properties. Clayton South, Australia: CSIRO Publishing, pp. 89-113.

Soil Survey Division Staff (1993) Soil survey manual. Soil conservation service. In: U.S. Department of Agriculture handbook, 18 p.

Stenberg, B., Viscarra Rossel, R.A., Mouazen, A.M., Wetterlind, J. (2010). Visible and Near Infrared Spectroscopy in Soil Science. In: Advances in Agronomy, Elsevier, pp. 163–215. DOI: https://doi.org/10.1016/S0065-2113(10)07005-7

Tian, Y., Zhang, J., Yao, X., Cao, W., Zhu, Y. (2013) Laboratory assessment of three quantitative methods for estimating the organic matter content of soils in China based on visible/near-infrared reflectance spectra. Geoderma, 202–203, 161–170. DOI: https://doi.org/10.1016/j.geoderma.2013.03.018

Turco, M., Llasat, M.-C., von Hardenberg, J., Provenzale, A. (2014) Climate change impacts on wildfires in a Mediterranean environment. Climatic Change, 125 (3–4), 369–380.

Verma, S., Jayakumar, S. (2015) Post-fire regeneration dynamics of tree species in a tropical dry deciduous forest, Western Ghats, India. Forest Ecology and Management, 341, 75–82. DOI: https://doi.org/10.1016/j.foreco.2015.01.005

Viscarra Rossel, R.A., Behrens, T. (2010) Using data mining to model and interpret soil diffuse reflectance spectra. Geoderma, 158 (1–2), 46–54. DOI: https://doi.org/10.1016/j.geoderma.2009.12.025

Viscarra Rossel, R.A., Walvoort, D.J.J., McBratney, A.B., Janik, L.J., Skjemstad, J.O. (2006) Visible, near infrared, mid infrared or combined diffuse reflectance spectroscopy for simultaneous assessment of various soil properties. Geoderma, 131 (1–2), 59–75. DOI: https://doi.org/10.1016/j.geoderma.2005.03.007

Yang, Y., Hu, X., Cao, X., Jin, T., Wang, Y. (2021) Medium-Term Effects of Different Wildfire Severities on Soil Properties: a Case Study of Hengduan Mountains, southwestern China. In IOP Conference Series: Earth and Environmental Science (Vol. 861, No. 6, p. 062021). IOP Publishing.

Yeo, I.K., Johnson, R.A. (2000) A new family of power transformations to improve normality or symmetry. Biometrika, 87 (4), 954–959. DOI: https://doi.org/10.1093/biomet/87.4.954

Zhang X.-Y., Sui Y.-Y., Zhang X.-D., Meng K., Herbert S.J. (2007). Spatial Variability of Nutrient Properties in Black Soil of Northeast China. Pedosphere, 17 (1), 19–29. DOI: https://doi.org/10.1016/S1002-0160(07)60003-4

Zheng, G., Ryu, D., Jiao, C., Hong, C. (2016) Estimation of Organic Matter Content in Coastal Soil Using Reflectance Spectroscopy. Pedosphere, 26 (1), 130–136. DOI: https://doi.org/10.1016/S1002-0160(15)60029-7

Zovko, M., Romić, D., Colombo, C., Di Iorio, E., Romić, M., Buttafuoco, G., Castrignanò, A. (2018) A geostatistical Vis-NIR spectroscopy index to assess the incipient soil salinisation in the Neretva River valley, Croatia. Geoderma, 332, 60-72. DOI: https://doi.org/10.1016/j.geoderma.2018.07.005